Enhanced transferrin modified targeting delivery system via AFP promoter MR imaging reporter gene transfection

Jiaping Zhou
Zhejiang University School of Medicine Second Affiliated Hospital
Qiaomei Zhou
Zhejiang University School of Medicine Second Affiliated Hospital
Gaofeng Shu
Zhejiang University College of Pharmaceutical Sciences
Xiaojie Wang
Zhejiang University School of Medicine Second Affiliated Hospital
Yuanfei Lu
Zhejiang University School of Medicine Second Affiliated Hospital
Haiyan Chen
Zhejiang University School of Medicine Second Affiliated Hospital
Tingting Hu
Zhejiang University School of Medicine Second Affiliated Hospital
Jinsong Cai
Zhejiang University School of Medicine Second Affiliated Hospital
Yongzhong Du
Zhejiang University College of Pharmaceutical Sciences
Risheng Yu (risheng-yu@zju.edu.cn)
Zhejiang University School of Medicine Second Affiliated Hospital https://orcid.org/0000-0003-0554-9484

Research

Keywords: AFP promoter transfection, magnetic resonance imaging (MRI), transferrin, targeted drug delivery, hepatocellular carcinoma

Posted Date: March 25th, 2020

DOI: https://doi.org/10.21203/rs.3.rs-18859/v1

Abstract

Background: Effective treatment and early diagnosis is essential for patients with hepatocellular carcinoma. Nowadays, there is an increasing interest in the utilization of AFP/Fth as an endogenous contrast agent for the early diagnosis of liver cancers. The transfection of AFP/Fth also leads to a considerable upregulation of transferrin receptors (TfR), which might be a potential target for an enhanced delivery of nanomedicines. However, there is no information regarding the utilization of overexpressed TfR for the treatment of liver cancers. Thus, the objective of our study was to investigate whether the transfection of AFP/Fth could be used for the early diagnosis, but also for an enhanced treatment of live cancers.

Results: It was found that both of ferritin and TfR were upregulated after the transfection of AFP/Fth plasmid. The transfected cells showed a higher uptake of ferric ion than the un-transfected ones, resulting in a lower T2WI intensity. This result was due to the upregulation of ferritin in transfected cells, suggesting that transfection of AFP/Fth plasmid could be a potential strategy for early diagnosis of liver cancer. As compared with the un-transfected cells, the transfected cells showed a higher uptake of transferrin-modified liposomes, which was due to the specific interaction between transferrin with TfR overexpressed on the transfected cells. This is also the reason why the transferrin modified doxorubicin loaded liposomes (Tf-LP/DOX) showed better in vitro and in vivo anticancer ability than the LP/DOX. This results also suggested that transfection of AFP/Fth could result in an enhanced therapy of liver cancer.

Conclusions: Transfection of AFP/Fth could be used for the early diagnosis, but also for an enhanced treatment of live cancers.

Background

Liver cancer is one of the most common cancers in the world, which is the sixth most common cancer and the second leading cause of cancer mortality worldwide [1, 2]. Although with the development of treatment management, the five-year survival rate for liver cancer has gradually increased, the incidence and mortality of liver cancer is still rising steadily [3–8]. Meanwhile, due to the lack of early diagnosis, many patients are advanced and have severely impaired liver reserve when they first visit, in which stage patient loss the opportunities of radical surgery or transcatheter arterial chemoembolization (TACE) [2, 8, 9]. In this situation, chemotherapy is still an important therapeutic approach [10–13]. and at the same time shows that early diagnosis and effective follow-up treatment of hepatic cancer are effective strategies to improve prognosis [1, 2].

Magnetic resonance imaging (MRI) is an important imaging examination in the diagnosis of liver cancer, which provides multiparameter imaging and exhibits the advantages of high spatial resolution, soft tissue resolution without ionizing radiation [14–16]. Modern molecular imaging can supply early tumor diagnosis, which used novel reporter genes for MRI gene expression, including ferritin, transferrin receptor, β-galactosidase, and tyrosinase [14, 15, 17]. As an endogenous contrast agent, ferritin reporter gene

shows no cellular toxicity and can persistently produce a reduction of the signal intensity in MRI without fading over time comparing with exogenous contrast agents [18–20]. As a molecular imaging reporter gene, ferritin heavy chain (Fth) was one major candidate regulator of ferritin activity [21, 22]. And several studies have reported the diagnosis results of ferritin reporter gene [14, 22–24]. However, no research has been reported about the targeted therapy efficiency following the upregulated surface receptor caused by Fth transfection.

Alpha-fetoprotein (AFP) is a primitive embryonic protein, which is expressed positively in 80% of hepatocellular carcinoma and some embryonal tumors [25]. Therefore, as a serum tumor marker of HCC, its elevation often indicates the presence of HCC [25, 26]. Utilize the specific expression of AFP in hepatocellular carcinoma to introduce the plasmid which concluded an AFP promoter and Fth as subsequent genes. Promote the expression of follow-up ferritin gene for early diagnosis [25, 27].

Transferrin receptors are overexpressed on the surface of cancer cells compared to the normal cells because of the rapid proliferation and the increased iron demand in malignant tumor [28–30]. It was said that the number of TfR on their surface is 100-fold higher than that of normal cells [31]. Transferrin is also an indispensable component, and the most basic physiological function of transferrin is to bind and transport ferric ions, thereby controlling the level of free iron in the body fluid [32]. Combine with the upregulation of TfR promoted by ferritin expression, transferrin is considered as the most suitable ligand for targeting drugs delivery into cancer cells [29–31].

Doxorubicin is widely used in clinical treatment due to its broad antitumor spectrum [21, 33]. However, while killing tumor cells, doxorubicin also produces serious adverse reactions, such as cardiotoxicity, bone marrow suppression, etc., inducing the low therapeutic index and limited clinical application [21, 33–35]. It is necessary to encapsulate doxorubicin in the drug carrier to increase the accumulation of drug at lesion site and reduce the distribution to normal tissues. Liposomes have many advantages of non-toxicity, stability, biodegradability and economic feasibility [36, 37]. Liposomes enter the blood circulation through various channels, and most of the liposomes entering the blood circulation are selectively distributed in the reticular endothelial cells rich in phagocytes, leading to a significant increase in the total retention of encapsulating drugs in some organs, especially the liver and spleen and less into the bone marrow, myocardium and nerve tissue[37]. As mentioned above, the modified doxorubicin loaded liposomes are hoping to enhance the active targeting ability and further reduce the toxic and side effects [38–40].

Previously, the performance of AFP/Fth as an MRI reporter gene in AFP-positive cells was assessed [41], where indicated AFP/Fth appeared to be a promising endogenous contrast agent. In this paper, the influence of AFP/Fth on subsequent anti-tumor treatments while early molecular imaging was assessed. Although transferrin modified doxorubicin liposomes are not lack of reports [42, 43], we use them to evaluate subsequent targeting efficacy. MRI reporter gene as contrast agent has almost no biotoxicity, and the therapeutic potential of the drug improved at the same time as early diagnosis, which provides more possibilities for more efficient targeted therapy in the future.

In this study, we verified the dual-role of endogenous ferritin reporter gene, which decreased the T2WI intensity and investigated the targeted therapy efficacy of transferrin-modified doxorubicin liposomes (Scheme 1). The process of how AFP/Fth result in T2WI signal change included the specific express choice of plasmid, the overexpression of ferritin, the up-regulation of receptor and the improved iron uptake level. Further, several types of liposomes were prepared, and were used to test the following targeting ability and anti-tumor effect in transfected HepG2 cells and transfected subcutaneous liver cancer model.

Results And Discussion

^{1}H NMR spectroscopy of DSPE-PEG-Mal-Tf

The synthesis scheme of A54-PEG-SA is shown in Scheme 2. To identify the junction between transferrin ligand and 1,2-distearoyl-sn-glycero-3-phosphoethanolamine PEG Maleimide (DSPE-PEG-Mal), we performed ^{1}H NMR spectra with chloroform-d. As shown in Figure 1A, the peaks at about 3.57 ppm in the spectrum pf DSPE-PEG-Mal was belonging to the proton of -PEG, and the peaks at about 6.60-6.70 ppm belonging to the proton of -maleimide. Peaks at 3.57 ppm attributed to -PEG were also observed in the spectrum of DSPE-PEG-Tf, and at the same time, while the proton peak of maleimide (6.60-6.70 ppm) at the composition could not be observed, which indicated that maleimide was linked. Together, these results demonstrate the successful synthesis of DSPE-PEG-Tf.

Scheme 2. Synthetic Scheme of DSPE-PEG-Tf

Synthesis and characterization of LPs, Tf-LPs, LP/DOX, Tf-LP/DOX

Liposomes were prepared by membrane ultrasound and doxorubicin encapsulation via ammonium sulfate gradient method. The particle size and size distribution of liposomes were measured by dynamic light scattering (DLS) (Table 1). As shown in Figure1B-E, the average particle sizes of blank liposomes (LPs) and transferrin modified liposomes (Tf-LP) were 83.97±4.79 nm and 91.25±7.39 nm, respectively. On the other hand, doxorubicin loaded liposomes (LP/DOX) and transferrin modified liposomes loaded with doxorubicin (Tf-LP/DOX) were 62.58±5.69 nm and 48.05±7.76 nm, respectively. TEM examinations showed that each type of liposomes had a hollow spherical morphology, and their average particle sizes were similar to those measured by DLS. These results suggested that the average particle size of liposomes could be reduced by encapsulating them within the anti-cancer drug of DOX, which could be due to the intermolecular interaction. It should be noted that liposomes with size< 80 nm are effective at delivering the drug into lesion sites, which could provide an excellent anticancer capability [43].

Drug loading, encapsulation efficacy and Drug release

Then, the drug loading (DL) and encapsulation efficacy (EE) of liposomes were quantified by a fluorescence spectrophotometer via a centrifugal ultrafiltration method. As displayed in Table 1, both of LP and Tf-LP had a high DOX encapsulation efficiency, which was 88.11±3.39% and 93.82±1.28%, respectively. The drug loading of LP and Tf-LP were calculated to be 9.85±0.69% and 10.26±0.72%, respectively. The drug release profiles suggested that free DOX exhibited a rapid release behavior, with approximately 100% of DOX was released within 10 h (Figure 1F). In comparison, Tf-LP/DOX had a proper sustained release profile, with 89.8% of DOX was released within 24h. We also found that the drug release behavior of Tf-LP/DOX was quite similar to that of LP/DOX, suggesting that the transferrin modification slightly influenced the drug release performance of liposomes.

Table 1. Particle Diameter and Zeta Potential of blank LP, TF-LP, LP/DOX, Tf-LP/DOX. Drug loading, encapsulation efficacy of LP/DOX and Tf-LP/DOX.

Figure 1. (A) ^{1}H NMR of DSPE PEG-Tf the major peaks were pointed out; (B)The size distribution and morphology of LPs; (C) The size distribution and morphology of Tf-LP; (D) The size distribution and morphology of LP/DOX; (E) The size distribution and morphology of Tf-LP/DOX; (F) Drug release of free DOX, LP/DOX, Tf-LP/DOX.

AFP specific expression and AFP promoter drives Fth expression in AFP-positive cells

The expression levels of AFP protein in HepG2 and LO2 cells were verified by western blot analysis. The results showed that LO2 cells had a lower amount of APF protein as compared with HepG2 cells (Figures 2A and 2C). As the expression level of AFP protein is a good indicator of AFP activity [25], HepG2 cells were considered AFP positive, while LO2 cells were considered as AFP-negative in this study. The above result demonstrated the feasibility of AFP as the promoter in AFP/Fth plasmid and provide the basis for the subsequent verification test.

To examine whether transfected by the plasmid which contains ferritin heavy chain at the same time with AFP as a promoter caused ferritin overexpression, western blot was performed. As presented in Figures 2B and 2D, the expression level of ferritin in HepG2 with transfection was significantly higher than those without transfection. On the other hand, transfection for 48 h resulted in a higher amount of ferritin expressed in HepG2 cells than those for 24 h. These results have supported that ferritin could be overexpressed after the liver cancer cells were transfected with AFP/Fth. Transfection for 48h as a key time point was then chosen for the following studies.

Specific upregulation of TfR

To examine the effects of AFP/Fth transfection time (24 and 48h) on the TfR expression level, hepatoma carcinoma cells (HepG2) were transfected with or without ferritin reporter gene and observed through a laser confocal microscope via an immunofluorescence method. Apparently, TfR was specifically up-regulated in transfected hepatoma carcinoma cells, as evidence showing that the green fluorescence intensity of transfected HepG2 was much stronger than that of untransfected one (Figure 2E). It was also found that the HepG2 transfected with ferritin reporter for 48 h had a higher fluorescence intensity than those transfected for 24 h, indicating that the expression level of TfR could be increased after transfection and showed a more satisfied expression with a proper prolonged transfection time. Collectively, these growing evidences demonstrated that the AFP / Fth plasmid induced the upregulation of TfR on its cell surface after transfection, providing a basis for subsequent targeted therapy.

The signal decreased effect in MRI

The collected cells were subjected to MR imaging to study the contrast imaging effect caused by changed iron uptake ability via AFP/Fth transfection. It was observed in all three groups (non-transfection HepG2 cells group, 24h-transfection HepG2 cells group, 48h-transfection HepG2 cells group) that cells supplemented with an extra FAC concentration resulted in a significant decrease in the signal intensity. It can be explained that on the basis of regulation of transferrin receptors on cancer cell surface, the extra FAC supplement leaded to more cellular iron accumulation, which caused the T2WI intensity signal decline. The growing results of T2-/T2*-WI also suggested that the signal intensity of 24h/48h-transfection HepG2 cells were significantly lower than those without transfection, whether FAC or not (Figure 2F). These phenomena maybe induced by the ferritin overexpression and transferrin receptor upregulation in hepatoma cells after AFP/Fth plasmid transfected. On the other hand, 48h-transfection HepG2 cells group further showed lower signal intensity than those 24h-transfection. It was indicated that 48-hour transfection give rise to a more receptor overexpression possibility so that more iron could be transported into the cell, compared to 24-hour transfection. The quantitative analysis according to the region of interest (ROI=8px) of the T2*WI were analyzed and showed in Figure 2G and 2H. This serial of analysis confirmed that as shown in previous transfection experiments, ferritin overexpression, transferrin receptor up-regulation could lead to the intracellular iron accumulation in the condition of FAC provided, which then bring about the lower T2WI intensity.

Figure 2. (A) Western Blot for AFP of LO2 and HepG2 cells; (B) Western Blot for ferritin of different transfection duration; (C) quantitative values of AFP expression in LO2 and HepG2 cell (*$p < 0.05$, vs LO2 cell group n = 3); (D) quantitative values of ferritin expression in HepG2 cells transfected for 24h, 48h, comparing to untransfected $HepG_2$ cells (***$p<0.001$, vs $HepG_2$ cell group and transfection for 24h group, n=3); ; (E) immunofluorescence for observation that TfR upregulation of HepG2 cells untransfected and transfected for 24h, 48h. (F) MRI for HepG2 cells untransfected or transfected for 24h, 48h; with or

without FAC (c=0.5mM) provided; (G) Quantitative T2WI signal intensity analysis of HepG2 cells that unsupplied with FAC untransfected or transfected for 24h, 48h; (H) Quantitative T2WI signal intensity analysis of HepG2 cells that provided with FAC untransfected or transfected for 24h, 48h (**p<0.01, ***p<0.001, vs HepG2 cell group and transfection for 24h group, n=3).

Cellular uptake of transferrin modified particles in HepG2 cells

The cellular uptake of liposomes was observed by a fluorescence inverted microscope. A fluorescence dye of FITC was used to label the blank and target-modified liposomes, which was abbreviated as LP_{FITC} and Tf-LP_{FITC}, respectively. As shown in Figures 3A and 3B, both of transfected and untransfected HepG2 cells showed a gradual increase in fluorescence intensity as the incubation time was increased, suggesting that the cellular uptake of liposomes was time dependent. Looking deeply, transfected HepG2 cells treated with Tf-LP_{FITC} had a stronger fluorescence intensity than those treated with $LP_{FITC,}$ indicating that transferrin-modification could remarkably increase the uptake of liposomes. However, this behavior was not observed in the untransfected HepG2 cells, suggesting that transferrin-modification could specifically target the liposomes to the transfected cells, rather than the untransfected ones. As we mentioned previously, transferrin receptors were largely upregulated on the surface of HepG2 cells after the cells were transfected. The transferrin on the surface of liposomes could specifically target the transferrin receptors, thereby leading to the observation that a higher number of Tf-LP_{FITC} were uptake by the transfected HepG2 cells. Previous research also reported that the transferrin modified nanoparticles have a similar specific homing function for tumor cells that owned abundant TfR to mediate the cellular uptake of drugs [28, 44, 45].

The cytotoxicity of various liposomes

The toxicity of liposomes loaded with or without Dox was investigated via an MTT assay, in which HepG2 cells with or without transfection were used. As revealed in Figure 3C, LPs and Tf-LP showed little toxicity to cells at the tested concentration of10-100 μg/ml. Subsequently, we examined the toxicity effects of Tf-LP/DOX and LP/DOX toward HepG2 cells with or without transfection, in which DOX was used as positive controls. In general, all of the three liposomes reduced the cell viability with increasing the DOX concentration, in which free DOX exhibited the best anti-cancer efficiency (Figures 3D and 3E). In the case of HepG2 without transfection, Tf-LP/DOX and LP/DOX showed a similar ability to kill the cancer cells at the same dose of DOX. For the transfected HepG2 cells, the viability of cells treated with Tf-LP/DOX was clearly lower than those treated with LP/DOX at DOX concentrations of 2-4 μg/ml, which suggested that transferrin modification endows liposomes with a greater anticancer efficiency.

Figure 3. (A) Fluorescence images of untransfected and transfected HepG2 cells incubated with LP_{FITC} and Tf-LP_{FITC} for 0.5 h, 2 h, 6.0 h and 12.0 h, respectively (scale bar=50μm); (B) The quantitative analysis

of fluorescence signals, (*p < 0.05 , **p < 0.01 and ***p < 0.001, n = 3); (C) Cell viability was measured for HepG2 cells incubated for with LPs and Tf-LP at various doses for 24h; (D) Cell viability was measured for HepG2 cells incubated for 24 h with LP/DOX and Tf-LP/DOX at various doses for 24h; (E) Cell viability was measured for HepG2 cells that transfected for 48h and then incubated for with LP/DOX and Tf-LP/DOX at various doses for 24h; **p<0.01, (***p<0.001, vs free DOX group, n=6).

Western blotting for tumor transfection

To further verify the targeting expression of Fth in AFP positive hepatocellular carcinoma, the expression level of ferritin was studied via the western blotting method. As shown in Figure 4A, the transfection induced a higher expression level of Fth observed in tumor as compared to liver tissue, which should be mainly attributed to the active targeting ability of Tf-LP/DOX. The quantitative data in Figure 4B also showed that the expression level of Fth protein in transfected tumor was much higher than that in liver and non-transfected tissues, which was in accordance with the easier results obtained in western blotting analysis of cells.

Targeting ability of transferrin modified particles in vivo.

In vivo targeting ability of transferrin-modified liposomes was investigated by intravenously injected the mice with ICG-labeled Tf-LP (Tf-LP/ICG) or LP/ICG. After 24h and 48h of injection, the fluorescence images of major organs and tumors were captured, followed by quantifying the fluorescence intensity of tumors (Figures 4C and 4D). It was shown that the liposomes were mainly accumulated in the liver and tumor. The fluorescence signal of Tf-LP/ICG in tumor collected in transfected mice was significant stronger than that of transfected ones. Nevertheless, the tumor of mice treated with LP/ICG showed significant differences in fluorescence intensity, further verifying the enhanced targeting ability of transferrin-modified liposomes to transfected AFP positive hepatoma carcinoma cell. These results were nearly consistent with those obtained in cellular uptake.

Figure 4. (A) The ferritin expression in liver and tumor of transfection groups were measured by Western Blot assay; (B); The quantitative analysis of protein bands, *p < 0.05 and **p < 0.01 vs untransfected group, n = 3; (C) Biodistribution of LP/ICG and Tf-LP/ICG in vivo at 24h and 48h; (D) Quantitative analysis of fluorescence intensity in tumors (n = 3).

The anti-tumor effects

To confirm the therapeutic efficacy of Tf-LP/DOX to the HepG2 cell subcutaneous hepatoma model, we randomly divided the model mice for 6 groups (Figure 5A), and administrated for every 5 days (Figure 5B)

with a single dose of 4mg/Kg according to the mean weight of each group via tail vein injection. It should be noted that intratumor injection transfection was given two days prior to treatment for two of the group (Figure 5A). As shown in Figure 5C, the saline group showed a rapid tumor growth, with the relative tumor volume multiplied 22.37- fold within 25 days. In contrast, administration of doxorubicin loaded liposomes could effectively inhibit the tumor growth to a certain extent. It should be noted that Tf-LP/DOX showed the highest efficiency in term of inhibiting tumor growth of the transfection group, which was similar to that of free DOX. At day 25, the final relative tumor volume (RTV) in Tf-LP/DOX of transfection group was notably lower than Tf-LP/DOX of non-transfection group and LP/DOX of transfection group. Meanwhile, fluctuations in body weight in mice during the treatment were an indirect reflect of the safety of the treatment. As shown in Figure 5D, the body weights of mice treated with free DOX significantly decreased, which was on account of its systemic toxicity. Besides the similar results as cytotoxicity experiments, Tf-LP/DOX showed surprising anti-tumor effects after transfection, and its efficacy was even beyond free doxorubicin, which could be explained as the tumor microenvironment was more suitable for Tf-LP / DOX to accumulate and free doxorubicin had no targeting property in vivo in the meantime.

Histological analysis

Anti-tumor effect and side effects of different drugs on important organs during drug administration were observed through H&E staining. The anti-tumor extent was presented in Figure 5E, a multitude of tumor cells were destroyed in Tf-LP/DOX of transfection group. No obviously serious myocardial damage was observed in all groups, which may cause by the short administration period [34].

Figure 5. (A) The plasmid injection and drug injection schedule., respectively; (B) Groups during treatment; (C) Tumor growth curve after injected with various drug with 25 days,*$p<0.05$ and **$p<0.01$,vs Tf-LP/DOX (transfected group), n=5; (D) Body weight change curve of the mice; (E) Representative H&E sections of tumor tissue of mice after treatment with various drug.

Conclusion

In summary, we confirmed the dual effects that early diagnosis of hepatocellular carcinoma in molecular-level and subsequent intensive treatment via AFP/Fth transfection. AFP / Fth can be specifically promoted in AFP-positive cells, such as HepG2 cells. The subsequent consequence that T2WI intensity values significantly reduce, indicating well for early diagnosis of hepatocellular carcinoma. Meanwhile, the upregulation of TfR attracted a significantly increased amount of Tf-LP/DOX, which means a better targeting ability and anti-tumor efficacy of transferrin modified liposomes emerged to transfected AFP positive hepatoma carcinoma cell comparing to untransfected ones. Hence, the transfection of the AFP/Fth gene achieved the early diagnosis of hepatocellular carcinoma, and another promising role that

made Tf-LP/DOX or other transferrin functionalized preparations to be a more efficient and safer approach for subsequent treatment.

Materials And Methods

Hydrogenated soybean phospholipid (HSPC) was purchased from Advanced Vehicle Technology L.T.D. Co, Ltd (Shanghai, China), Human holo Transferrin (T4132), Branched PEI (25kD) were obtained from Sigma-Aldrich Inc (St. Louis, MO, USA). Cholesterol, 1,2-distearoyl-sn-glycero-3-phosphoethanolamine PEG Maleimide (DSPE-PEG-Mal), Tris (2-carboxyethyl) phosphine Hydrochloride (TECP), Doxorubicin hydrochloride (Dox), 3-(4,5-dimethylthiazol-2-yl)-2,5-diphenyltetrazolium bromide (MTT), fluorescein isothiocyanate (FITC) were purchased from Aladdin Reagent Database Inc (Shanghai, China). 2-Iminothiolane hydrochloride (Traut's reagent) was purchased from Yuanye Bio-Technology Co, Ltd (Shanghai, china). 4',6–15 diamidino-2-phenylindole (DAPI) was purchased from Beyotime Biotechnology (Shanghai, China). Indocyanine green (ICG) was obtained from Tokyo Chemical Industry Co, Ltd (Tokyo, Japan). Octadecylamine (ODA, 95%) was purchased from Fluka, USA. The AFP/Fth plasmid, encoding an AFP promoter and ferritin heavy chain, was synthesized by Shanghai Genechem Co, Ltd (Shanghai, China) according to the Fth gene sequence in GenBank (NM_013233). Antibodies including anti-AFP antibody and anti-ferritin heavy chain antibody were purchased from Abcam (Abcam, Cambridge, UK, ab65080). All other chemicals and solvents were of analytical or chromatographic grade. Deionized water (18.4 MΩ cm) used in all experiments was prepared using a Milli-Q system (Millipore, Boston, USA) and was used in all experiments.

Cell culture

HepG2 cell and LO2 cell were obtained from Chinese Academy of Sciences cell bank (Shanghai, China). HepG2 cell line was AFP positive human hepatocellular carcinoma cell,LO2 cell line was human hepatocytes. Cell was cultured in Dulbecco's Modified Eagle Medium (Gibco, USA) supplemented with 10% FBS (Gibco, USA) and 1% penicillin–streptomycin (Gibco, USA) in a 37 °C incubator with 5% CO2. Cells were subcultured regularly using trypsin/EDTA (Meilune, China).

Mice

BALB/C nude female mice aged 4–5 weeks had 16 ± 2 g weights and were obtained from Zhejiang Medical Animal Centre (Hangzhou, China), which were housed with free access to water and food. All the animal experiments were in line with the ARRIVE guidelines and were carried out in according to National Institutes of Health (NIH, USA) protocols, approved by the guidelines of Ethical Committee of Zhejiang University.

Synthesis of transferrin functionalized DSPE-PEG-Mal (DSPE-PEG-Tf)

DSPE-PEG2000-Tf was synthesized as has been reported, transferrin and the EDTA boric acid buffer containing traut's reagent were mixed to incubated in the dark for 1 h on a rotational shaker at 110 rpm, and then dialyzed overnight in a 0.1 mM TCEP solution, which was as a dialysis external fluid, to separate the excessive traut's reagent. Then the thiolated transferrin was added into the DSPE-PEG-Mal solution drop by drop, reacting for 8 hours under the water bath 37 °C with gently agitation, which is connected with the reaction of mercapto and amino actually. Eventually, dialyzed for purification to obtain the DSPE-PEG_{2000}-Tf [46].

^{1} H NMR measurement of DSPE-PEG-Tf

The composition and structure of DSPE-PEG-Tf were confirmed by 1H-NMR Spectroscopy. Dissolve the same amount of DSPE-PEG-Mal, transferrin and DSPE-PEEG-Tf in 0.7 ml Chloroform-d in NMR tubes, respectively. The 1H NMR spectra were recorded using a 400-MHz spectrometer (Inova 400, Varian, USA) at 25 °C.

Preparation of transferrin modified doxorubicin liposomes

Liposomes were prepared using a slightly modified method according to a previously published method [43]. Briefly, the liposomes were prepared by using HSPC: cholesterol: DSPE-PEG2000-MAL at a molar ratio of 6:3:0.6. The lipids were dissolved in the mixture organic solvent of chloroform: methanol (2:1 v/v), and dried to a thin lipid film in a round-bottom flask on a rotary evaporator at 53℃. Then the formed lipid film was hydrated with ammonium sulphate buffer (250 mM, PH8.5) at 53℃. The monolayer liposomes were treated with Ultrasonic cell crusher (JY92-II, Ningbo Scientz Biotechnology Co, Lab). The obtained liposomes were then dialyzed to remove the non-entrapped ammonium sulphate. The liposomes were then extruded through the polycarbonate membrane of pore size 0.2 um for one time to make liposomes more homogeneous.

Doxorubicin was encapsulated into the liposomes using the ammonium sulfate gradient method. Briefly, the ammonium sulphate liposome suspension was served in a penicillin bottle in Water bath magnetic stirrer at 60 ℃. Subsequently, doxorubicin powder was added to the liposomes suspension to achieve a drug to PL ratio of 1/10(w/w). The solution was stirred at 60 °C softly for 1 h and then dialyzed in the deionized water to remove the free doxorubicin. The encapsulation of ICG was same as doxorubicin.

DSPE-PEG2000-Tf was added into doxorubicin loaded liposomes (LP/DOX) with slight agitation under 37 °C for an hour in addition to compound the transferrin modified liposome.

The preparation of FITC labeled liposomes (LP_{FITC}) were similar to the usual blank liposomes. Use HSPC: cholesterol: DSPE-PEG2000-Mal at a molar ratio of 6: 3: 0.6, including the FTIC-ODA of 5% quality of the total lipids. The following steps were as above.

Physical characterization of preparations and morphology

The particle size, and size distribution were measured by Dynamic light scattering (DLS, Zetasizer, Malvern Co., UK). The morphology of microspheres was observed by transmission electron microscopy (JEM-1200EX, JEOL, Japan). The morphologies of LPs, LP/DOX, Tf-LP and Tf-LP/DOX were observed by transmission electron microscopy. The samples were prepared as follow: 10 ul of appropriate diluted solution was dropped on the 200-mesh copper grid coated with carbon,excess solution was carefully absorbed by filter paper after 2 minutes. Then add an appropriate amount of uranium acetate dye on the copper grid, left for about 20 seconds before wiping and for observation.

Drug loading and encapsulation efficiency

Encapsulation efficiency (EE) and drug loading (DL) were determined by a centrifugal ultrafiltration method. Briefly, the liposome solution was disrupted by methanol and the total DOX content was quantified by a fluorescence spectrophotometer (F-2500, Hitachi Co, Japan) with the excitation wavelength set at 476 nm and the slit widths at 10 nm (excitation) and 5 nm (emission). Then, the unencapsulated DOX dissolved in water was separated through an ultrafiltration tube (MW: 3.5 kDa), and the content was measured again. DL and EE were calculated by the following formulas:

DL%= (total mass of drug -mass of unencapsulated drug)/mass of loaded liposomes × 100%

EE%= (total mass of drug - mass of unencapsulated drug)/total mass of drug × 100%

Drug release

The in vitro drug release from the liposomes was evaluated by dialysis using PBS (pH 7.4) as a dissolution medium. Briefly, 500 μl LP/DOX and Tf-LP/DOX were placed into a dialysis bag (MWCO 3.5 kDa, Spectrum Laboratories, Laguna Hills, Canada) and dialyzed against PBS under sinking conditions with Incubator shaker (HZ-8812S, Scientific and Educational Equipment Plant, Taicang, China) with 110 rpm at 37 °C. At predetermined time points, the media were collected and replaced with fresh buffer solution. The drug content in the release medium was detected by fluorescence spectrophotometer.

Western blotting for AFP and Ferritin expression

The ferritin expression was confirmed by Western Blot assay. HepG2 cell was incubated for 48 h after transfection, using 80 ul RIPA buffer that containing protease inhibitor (Sigma, USA) per well to lyse the cells in 6-well plate on ice for 30 minutes. After centrifuging and collecting the cells in EP tubes, the protein concentration was evaluated by the bicinchoninic acid assay. The protein solution was added to 5* loading buffer in a ratio of 4:1 and denaturated in boiling water bath for 15 minutes. Then the samples were loaded onto 12% gels for SDS-PAGE. The cut gels which including the molecular weight between 21KD (ferritin heavy chain) and 42KD (β-actin) were transferred onto PVDF membranes for blotting. The membranes were blocked in 5% skim milk powder solution for 2 h at 37 °C and then incubated overnight at 4 °C with rabbit anti-Ferritin monoclonal antibody (1:2000, Abcam), the membranes were incubated with horseradish peroxidase-conjugated goat anti-rabbit IgG (1: 5000, Boster) for 1 h after thoroughly washing with TBST buffer. Eventually, the interest proteins were visualized using by enhanced chemiluminescent (ECL).

The confirmation of AFP expression was similar with ferritin' s, while AFP samples were loaded onto 15% gels for SDS-PAGE and incubated with anti-AFP monoclonal antibody (1:2000, Abcam) overnight.

Immunofluorescence assay for TfR expression

Cells were cultured in the 24-well plate containing coverslips for 24 hours before transfection. After 48 h post-transfection, the cells were washed with PBS and then fixed by 4% paraformaldehyde (PFA) for 10 min. Immediately after the fixation, use 5% normal goat serum for blocking at 37 °C for 1 h. To verify the up-regulation of transferrin receptor (TfR), the cells were incubated with a rabbit anti-TfR monoclonal antibody (1:100, Abcam, UK) at 4 °C overnight and then incubated with a DyLight 488-conjugated goat anti-rabbit secondary antibody (1:200, Boster, USA) for 1 h. The cell nucleus was counterstained with DAPI (1:1000, Beyotime, China). Then the coverslips were removed from the plate, fixed on glass slides, and finally examined under a laser confocal microscope (Olympus, Japan).

MRI study in vitro

Vitro MRI was further used to examine the effect of Fth gene transfection. 12 h after transfection, FAC with concentrations of 0.5 mM was added to cultured medium of FAC (+) group and co-incubate with cells for 12 h and 36 h respectively. After thorough washing with PBS thrice to remove free iron, cells were fixed in 4% PFA for 10 min and dissociated with trypsin, followed by suspending in 10 ul PBS in EP tubes and filled with 30 ul 1% un-solidified agarose solution each tube [22, 41]. T2*-weighted imaging (T2*WI), T2WI, T2 value and SI value were acquired using T2 fast spin echo and ESWAN sequences by a 3.0-T MR (GE Discovery MR750, USA). FSE sequence: repetition time (TR) = 3070.0 ms, echo time (TE) = 96.6 ms, and slice thickness = 1.0 mm; ESWAN sequence: TR = 52.3 ms, TE = 6.5–30.2 ms, and slice thickness = 1.0 mm.

Cellular uptake of transferrin modified particles in vitro.

In order to investigate the targeting ability of Tf-LP/DOX toward transfected AFP positive cell line, cellular uptake of Tf-LP/DOX and LP/DOX on with or without transfection HepG2 cell line were observed. Cells cultured in 24-well plate were divided into two equal parts, one half wells were designed for transfection while the other half not. During the 48 post-transfection incubation, the same amount per well of Tf-LP/DOX and LP/DOX were added to the two-group cells, respectively, as the time from the end of the experiment was 0.5 h, 2 h, 4 h, 8 h, 12 h. Finally, the fluorescence signals insides the cells were examined by inverted fluorescence microscopy and were also semi-quantified by Image J.

The cytotoxicity of doxorubicin loaded liposomes and blank liposomes

Cells were planted in 96-well plate and cultured in a 37 °C incubator with 5% CO2 for 24 h. The transfection group continued to incubate for 42 h, rinsing with PBS, then the culture medium was replaced by 200 ul of fresh media containing serial dilutions of Tf-LP/DOX and LP/DOX, and the cells were cultured for 24 h. Then, 20 ul of a 5 mg/ml MTT stock solution was added to each well. Four hours

later, unreacted dyes were carefully removed by aspiration. 150 ul DMSO was added each well to dissolve the formazan crystals. After 10 min of low speed oscillation, the OD value was measured by a Microplate reader (Bio-Rad, Model 680, USA) at a wave length of 570 nm. Wells that contained only medium and cells without intervention were set as the control group. The LPs group and Tf-LP group were added to the wells respectively after culturing for 24 h and then measured.

Transfection in vivo

The equal amount of plasmid that have mixed with PEI for 30 minutes were given to the nude mice of transfected group two days before the drug was administered, and then intratumorally injected for transfection, which was set for 24 h and 48 h. Finally, the tumors were ground into a slurry for WB detection to observe the expression of ferritin, and the liver tissues were also used as a control [47].

Targeting ability of transferrin modified particles in vivo.

HepG2 cells (1×10^6 cells/0.2 ml) were injected subcutaneously into in the right axillary of the female BALB/C nude mice (Zhejiang University, Hangzhou, China) and 0.2 ml Tf-LP/ICG and LP/ICG were given to the different groups with the same concentration by tail vein injection when tumors' volume reached 100mm^3 approximately. The distribution in vivo will be observed through whole-body fluorescent imaging system at 24 h, 48 h respectively.

The anti-tumor effect in mice

After successful tumor modeling, mice bearing tumor about 100 mm^3 were used in this study, the nude mice were randomly divided into 6 groups of five to six (Fig. 5A). Two of the groups will be transfected, and Tf-LP/DOX and LP/DOX were administrated separately. Tf-LP/DOX and LP/DOX were also given to another two groups, but no transfection pretreatment was performed. The remaining two groups were the free doxorubicin group and the saline group. Each group of mice were administered every 5 days at a single dose of 4 mg/Kg according to the mean weight of each group via tail vein injection (Fig. 5B). The volume of the tumor and the body weight of the mice were monitored on the day of the next administration to observe the anti-tumor effect among transfection and non-transfection, preparation and free drug. At indicated times after injection, mice were sacrificed and the heart, liver, spleen, lung, kidney, tumor were excised instantaneously. After gently washing away the excess blood, the tissue sections were used for HE staining observation. The tumor volume was determined by the two bisecting diameters of each tumor, which represented the largest (a) and smallest (b) diameter(mm) of the tumors, respectively, and the volume was calculated using the formula 0.5X ($a*b^2$).

The histology

The tumor tissues were submerged into 10% formalin for 48 h, then embedded in paraffin. Then HE staining was used to analyze the pathological changes of important organs between different groups of nude mice, and to observe the pathological difference between the four preparation groups, the free drug

group and the physiological group. The microscopic images were observed under Leica fluorescence microscope.

Statistical analysis

All the quantitative data were shown as means ± standard deviation (SD) of three separate experiments. Discrepancies between two groups were conducted by Student's t test and one-way analysis of variance (ANOVA) was used for discerning discrepancies between multiple groups. A P-value < 0.05 was considered statistically significant. All statistical analyses were done using STATA software.

Declarations

Abbreviations

AFP: alpha fetoprotein; DAPI: 4',6-diamidino-2-phenylindole; FITC: fluorescein isothiocyanate; Fth: ferritin; TfR: transferrin receptor; HCC: hepatocellular carcinoma; ICG: indocyanine green; MRI: magnetic resonance imaging; TACE: transcatheter arterial chemoembolization

Acknowledgements

We would like to thank the members of Professor Du 's team (Pharmacy School of Zhejiang University) for their guidance and assistance in this study.

Author Contributions

Risheng Yu and Yongzhong Du conceived the project. Jiaping Zhou performed the in vitro experiments. Jiaping Zhou and Qiaomei Zhou performed and analyzed in vivo experiments. Jiaping Zhou, Xiaojie Wang and Yuanfei Lu analyzed the data. Tingting Hu and Jinsong Cai participated in magnetic resonance imaging. Jiaping Zhou, Gaofeng Shu and Haiyan Chen wrote the paper with input from all authors.

Funding

This work was funded by the Natural Science Foundation of Zhejiang province (LY18H180003) and the National Natural Science Foundation of China (General Program: 81571662).

Availability of data and materials

All data generated or analyzed during this study are included in this published article and its supplementary information files.

Ethics approval and consent to participate

All animal experiments were approved by the local IACUC and local authorities and under the European Union Directive 2010/63/EU on the protection of animals used for scientific purposes.

Consent for publication

Not applicable.

Competing interests

The authors declare that they have no competing interests.

References

1. Tang A, Hallouch O, Chernyak V, Kamaya A, Sirlin CB: **Epidemiology of hepatocellular carcinoma: target population for surveillance and diagnosis.** *Abdom Radiol (NY)* 2018, **43:**13-25.
2. Villanueva A: **Hepatocellular Carcinoma. Reply.** *N Engl J Med* 2019, **381:**e2.
3. Llovet JM, Montal R, Sia D, Finn RS: **Molecular therapies and precision medicine for hepatocellular carcinoma.** *Nat Rev Clin Oncol* 2018, **15:**599-616.
4. Siegel RL, Miller KD, Jemal A: **Cancer statistics, 2019.** *CA Cancer J Clin* 2019, **69:**7-34.
5. Cronin KA, Lake AJ, Scott S, Sherman RL, Noone AM, Howlader N, Henley SJ, Anderson RN, Firth AU, Ma J, et al: **Annual Report to the Nation on the Status of Cancer, part I: National cancer statistics.** *Cancer-Am Cancer Soc* 2018, **124:**2785-2800.
6. Zhou M, Wang H, Zeng X, Yin P, Zhu J, Chen W, Li X, Wang L, Wang L, Liu Y, et al: **Mortality, morbidity, and risk factors in China and its provinces, 1990-2017: a systematic analysis for the Global Burden of Disease Study 2017.** *Lancet* 2019, **394:**1145-1158.
7. Sia D, Villanueva A, Friedman SL, Llovet JM: **Liver Cancer Cell of Origin, Molecular Class, and Effects on Patient Prognosis.** *Gastroenterology* 2017, **152:**745-761.
8. Llovet JM, Villanueva A, Lachenmayer A, Finn RS: **Advances in targeted therapies for hepatocellular carcinoma in the genomic era.** *Nat Rev Clin Oncol* 2015, **12:**436.

9. Galle PR, Tovoli F, Foerster F, Worns MA, Cucchetti A, Bolondi L: **The treatment of intermediate stage tumours beyond TACE: From surgery to systemic therapy.** *J Hepatol* 2017, **67:**173-183.
10. Ikeda M, Morizane C, Ueno M, Okusaka T, Ishii H, Furuse J: **Chemotherapy for hepatocellular carcinoma: current status and future perspectives.** *Jpn J Clin Oncol* 2018, **48:**103-114.
11. Hartke J, Johnson M, Ghabril M: **The diagnosis and treatment of hepatocellular carcinoma.** *Semin Diagn Pathol* 2017, **34:**153-159.
12. Ikeda M, Mitsunaga S, Ohno I, Hashimoto Y, Takahashi H, Watanabe K, Umemoto K, Okusaka T: **Systemic Chemotherapy for Advanced Hepatocellular Carcinoma: Past, Present, and Future.** *Diseases* 2015, **3:**360-381.
13. Forner A, Reig M, Bruix J: **Hepatocellular carcinoma.** *Lancet* 2018, **391:**1301-1314.
14. Yang C, Tian R, Liu T, Liu G: **MRI Reporter Genes for Noninvasive Molecular Imaging.** *Molecules* 2016, **21**.
15. Haris M, Yadav SK, Rizwan A, Singh A, Wang E, Hariharan H, Reddy R, Marincola FM: **Molecular magnetic resonance imaging in cancer.** *J Transl Med* 2015, **13:**313.
16. Tsai LL, Grant AK, Mortele KJ, Kung JW, Smith MP: **A Practical Guide to MR Imaging Safety: What Radiologists Need to Know.** *Radiographics* 2015, **35:**1722-1737.
17. Sinusas AJ, Thomas JD, Mills G: **The future of molecular imaging.** *JACC Cardiovasc Imaging* 2011, **4:**799-806.
18. Layne KA, Dargan PI, Archer J, Wood DM: **Gadolinium deposition and the potential for toxicological sequelae - A literature review of issues surrounding gadolinium-based contrast agents.** *Br J Clin Pharmacol* 2018, **84:**2522-2534.
19. Ramalho J, Ramalho M: **Gadolinium Deposition and Chronic Toxicity.** *Magn Reson Imaging Clin N Am* 2017, **25:**765-778.
20. Cheng S, Mi R, Xu Y, Jin G, Zhang J, Zhou Y, Chen Z, Liu F: **Ferritin heavy chain as a molecular imaging reporter gene in glioma xenografts.** *J Cancer Res Clin Oncol* 2017, **143:**941-951.
21. Carvalho C, Santos RX, Cardoso S, Correia S, Oliveira PJ, Santos MS, Moreira PI: **Doxorubicin: the good, the bad and the ugly effect.** *Curr Med Chem* 2009, **16:**3267-3285.
22. Yang Y, Gong MF, Yang H, Zhang S, Wang GX, Su TS, Wen L, Zhang D: **MR molecular imaging of tumours using ferritin heavy chain reporter gene expression mediated by the hTERT promoter.** *Eur Radiol* 2016, **26:**4089-4097.
23. Ono K, Fuma K, Tabata K, Sawada M: **Ferritin reporter used for gene expression imaging by magnetic resonance.** *Biochem Bioph Res Co* 2009, **388:**589-594.
24. Hasegawa S, Furukawa T, Saga T: **Molecular MR imaging of cancer gene therapy: ferritin transgene reporter takes the stage.** *Magn Reson Med Sci* 2010, **9:**37-47.
25. Kim KI, Lee YJ, Lee TS, Song I, Cheon GJ, Lim SM, Chung JK, Kang JH: **In vitro radionuclide therapy and in vivo scintigraphic imaging of alpha-fetoprotein-producing hepatocellular carcinoma by targeted sodium iodide symporter gene expression.** *Nucl Med Mol Imaging* 2013, **47:**1-8.

26. Marrero JA, Feng Z, Wang Y, Nguyen MH, Befeler AS, Roberts LR, Reddy KR, Harnois D, Llovet JM, Normolle D, et al: **Alpha-fetoprotein, des-gamma carboxyprothrombin, and lectin-bound alpha-fetoprotein in early hepatocellular carcinoma.** *Gastroenterology* 2009, **137:**110-118.
27. Wu L, Johnson M, Sato M: **Transcriptionally targeted gene therapy to detect and treat cancer.** *Trends Mol Med* 2003, **9:**421-429.
28. Jhaveri A, Luther E, Torchilin V: **The effect of transferrin-targeted, resveratrol-loaded liposomes on neurosphere cultures of glioblastoma: implications for targeting tumour-initiating cells.** *J Drug Target* 2019, **27:**601-613.
29. Moghimipour E, Rezaei M, Kouchak M, Ramezani Z, Amini M, Ahmadi AK, Saremy S, Abedin DF, Handali S: **A mechanistic study of the effect of transferrin conjugation on cytotoxicity of targeted liposomes.** *J Microencapsul* 2018, **35:**548-558.
30. Bao W, Liu R, Wang Y, Wang F, Xia G, Zhang H, Li X, Yin H, Chen B: **PLGA-PLL-PEG-Tf-based targeted nanoparticles drug delivery system enhance antitumor efficacy via intrinsic apoptosis pathway.** *Int J Nanomedicine* 2015, **10:**557-566.
31. Szwed M, Wrona D, Kania KD, Koceva-Chyla A, Marczak A: **Doxorubicin-transferrin conjugate triggers pro-oxidative disorders in solid tumor cells.** *Toxicol In Vitro* 2016, **31:**60-71.
32. Gomme PT, McCann KB, Bertolini J: **Transferrin: structure, function and potential therapeutic actions.** *Drug Discov Today* 2005, **10:**267-273.
33. Carvalho FS, Burgeiro A, Garcia R, Moreno AJ, Carvalho RA, Oliveira PJ: **Doxorubicin-induced cardiotoxicity: from bioenergetic failure and cell death to cardiomyopathy.** *Med Res Rev* 2014, **34:**106-135.
34. Octavia Y, Tocchetti CG, Gabrielson KL, Janssens S, Crijns HJ, Moens AL: **Doxorubicin-induced cardiomyopathy: from molecular mechanisms to therapeutic strategies.** *J Mol Cell Cardiol* 2012, **52:**1213-1225.
35. Tahover E, Patil YP, Gabizon AA: **Emerging delivery systems to reduce doxorubicin cardiotoxicity and improve therapeutic index: focus on liposomes.** *Anticancer Drugs* 2015, **26:**241-258.
36. Bigdeli A, Palchetti S, Pozzi D, Hormozi-Nezhad MR, Baldelli BF, Caracciolo G, Mahmoudi M: **Exploring Cellular Interactions of Liposomes Using Protein Corona Fingerprints and Physicochemical Properties.** *Acs Nano* 2016, **10:**3723-3737.
37. Panahi Y, Farshbaf M, Mohammadhosseini M, Mirahadi M, Khalilov R, Saghfi S, Akbarzadeh A: **Recent advances on liposomal nanoparticles: synthesis, characterization and biomedical applications.** *Artif Cells Nanomed Biotechnol* 2017, **45:**788-799.
38. Chang JE, Shim WS, Yang SG, Kwak EY, Chong S, Kim DD, Chung SJ, Shim CK: **Liver cancer targeting of Doxorubicin with reduced distribution to the heart using hematoporphyrin-modified albumin nanoparticles in rats.** *Pharm Res* 2012, **29:**795-805.
39. Daeihamed M, Haeri A, Ostad SN, Akhlaghi MF, Dadashzadeh S: **Doxorubicin-loaded liposomes: enhancing the oral bioavailability by modulation of physicochemical characteristics.** *Nanomedicine (Lond)* 2017, **12:**1187-1202.

40. Abraham SA, Waterhouse DN, Mayer LD, Cullis PR, Madden TD, Bally MB: **The liposomal formulation of doxorubicin.** *Methods Enzymol* 2005, **391:**71-97.
41. Zhang Q, Lu Y, Xu X, Li S, Du Y, Yu R: **MR molecular imaging of HCC employing a regulated ferritin gene carried by a modified polycation vector.** *Int J Nanomedicine* 2019, **14:**3189-3201.
42. Barenholz Y: **Doxil(R)–the first FDA-approved nano-drug: lessons learned.** *J Control Release* 2012, **160:**117-134.
43. Li X, Ding L, Xu Y, Wang Y, Ping Q: **Targeted delivery of doxorubicin using stealth liposomes modified with transferrin.** *Int J Pharm* 2009, **373:**116-123.
44. Luo M, Lewik G, Ratcliffe JC, Choi C, Makila E, Tong WY, Voelcker NH: **Systematic Evaluation of Transferrin-Modified Porous Silicon Nanoparticles for Targeted Delivery of Doxorubicin to Glioblastoma.** *ACS Appl Mater Interfaces* 2019, **11:**33637-33649.
45. Jhaveri A, Deshpande P, Pattni B, Torchilin V: **Transferrin-targeted, resveratrol-loaded liposomes for the treatment of glioblastoma.** *J Control Release* 2018, **277:**89-101.
46. Anabousi S, Laue M, Lehr CM, Bakowsky U, Ehrhardt C: **Assessing transferrin modification of liposomes by atomic force microscopy and transmission electron microscopy.** *Eur J Pharm Biopharm* 2005, **60:**295-303.
47. Aung W, Hasegawa S, Koshikawa-Yano M, Obata T, Ikehira H, Furukawa T, Aoki I, Saga T: **Visualization of in vivo electroporation-mediated transgene expression in experimental tumors by optical and magnetic resonance imaging.** *Gene Ther* 2009, **16:**830-839.

Figures

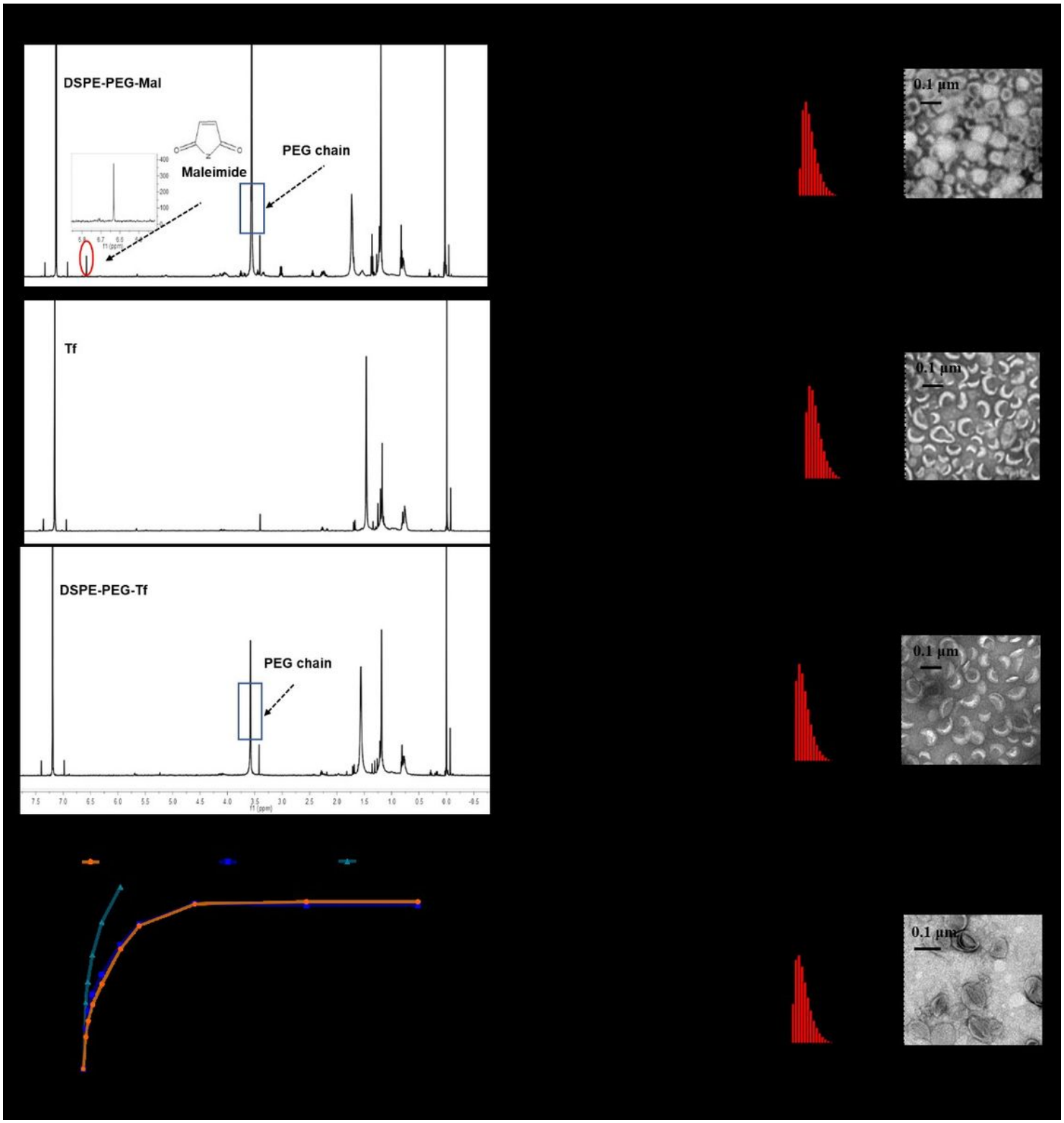

Figure 1

(A) 1H NMR of DSPE PEG-Tf the major peaks were pointed out; (B)The size distribution and morphology of LPs; (C) The size distribution and morphology of Tf-LP; (D) The size distribution and morphology of LP/DOX; (E) The size distribution and morphology of Tf-LP/DOX; (F) Drug release of free DOX, LP/DOX, Tf-LP/DOX.

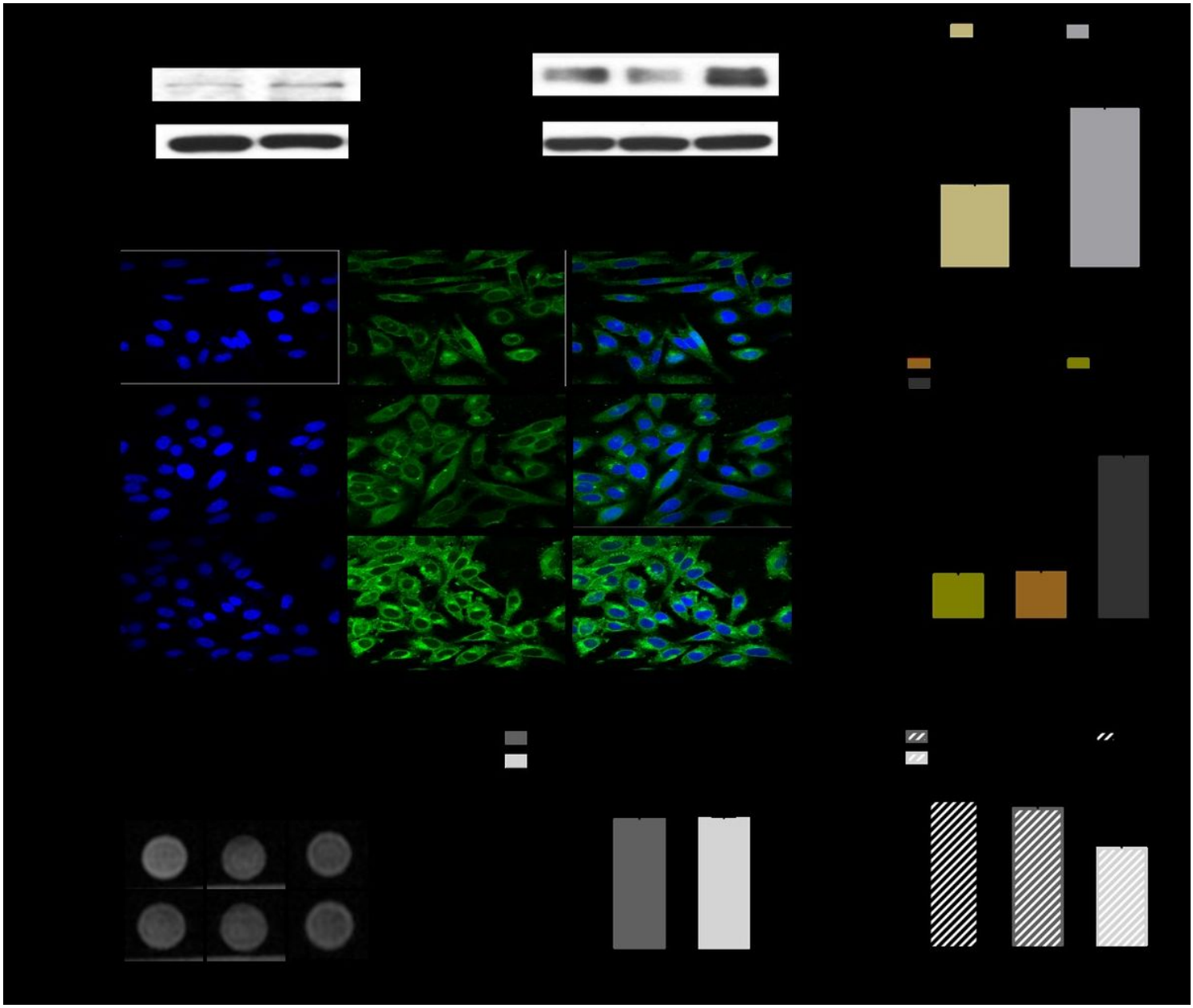

Figure 2

(A) Western Blot for AFP of LO2 and HepG2 cells; (B) Western Blot for ferritin of different transfection duration; (C) quantitative values of AFP expression in LO2 and HepG2 cell (*p < 0.05 , vs LO2 cell group n = 3); (D) quantitative values of ferritin expression in HepG2 cells transfected for 24h, 48h, comparing to untransfected HepG2 cells (***p<0.001, vs HepG2 cell group and transfection for 24h group, n=3); ; (E) immunofluorescence for observation that TfR upregulation of HepG2 cells untransfected and transfected for 24h, 48h. (F) MRI for HepG2 cells untransfected or transfected for 24h, 48h; with or without FAC (c=0.5mM) provided; (G) Quantitative T2WI signal intensity analysis of HepG2 cells that unsupplied with FAC untransfected or transfected for 24h, 48h; (H) Quantitative T2WI signal intensity analysis of HepG2 cells that provided with FAC untransfected or transfected for 24h, 48h (**p<0.01, ***p<0.001, vs HepG2 cell group and transfection for 24h group, n=3).

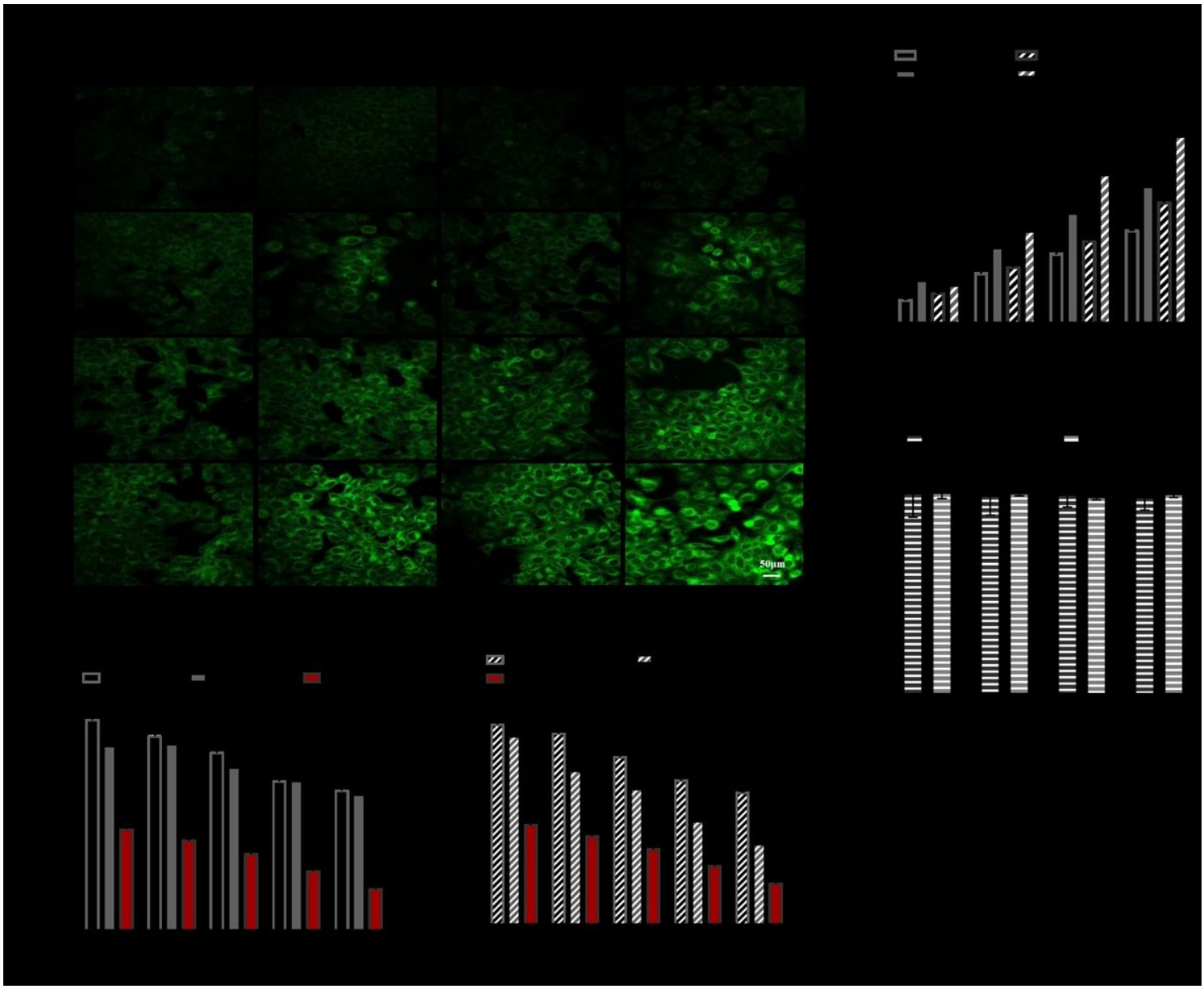

Figure 3

(A) Fluorescence images of untransfected and transfected HepG2 cells incubated with LPFITC and Tf-LPFITC for 0.5 h, 2 h, 6.0 h and 12.0 h, respectively (scale bar=50μm); (B) The quantitative analysis of fluorescence signals, (*p < 0.05 , **p < 0.01 and ***p < 0.001, n = 3); (C) Cell viability was measured for HepG2 cells incubated for with LPs and Tf-LP at various doses for 24h; (D) Cell viability was measured for HepG2 cells incubated for 24 h with LP/DOX and Tf-LP/DOX at various doses for 24h; (E) Cell viability was measured for HepG2 cells that transfected for 48h and then incubated for with LP/DOX and Tf-LP/DOX at various doses for 24h; **p<0.01, (***p<0.001, vs free DOX group, n=6).

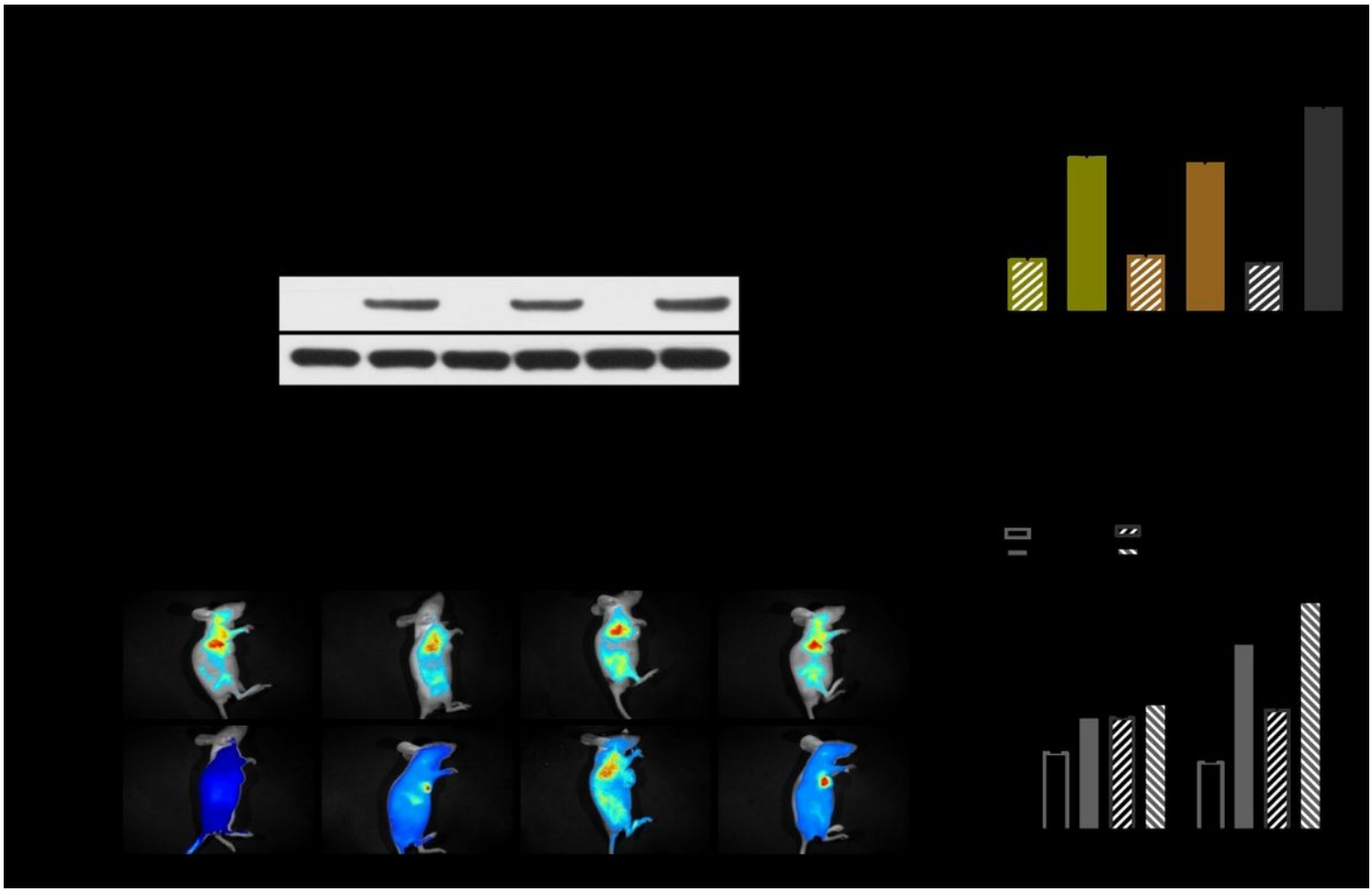

Figure 4

(A) The ferritin expression in liver and tumor of transfection groups were measured by Western Blot assay; (B); The quantitative analysis of protein bands, *p < 0.05 and **p < 0.01 vs untransfected group, n = 3; (C) Biodistribution of LP/ICG and Tf-LP/ICG in vivo at 24h and 48h; (D) Quantitative analysis of fluorescence intensity in tumors (n = 3).

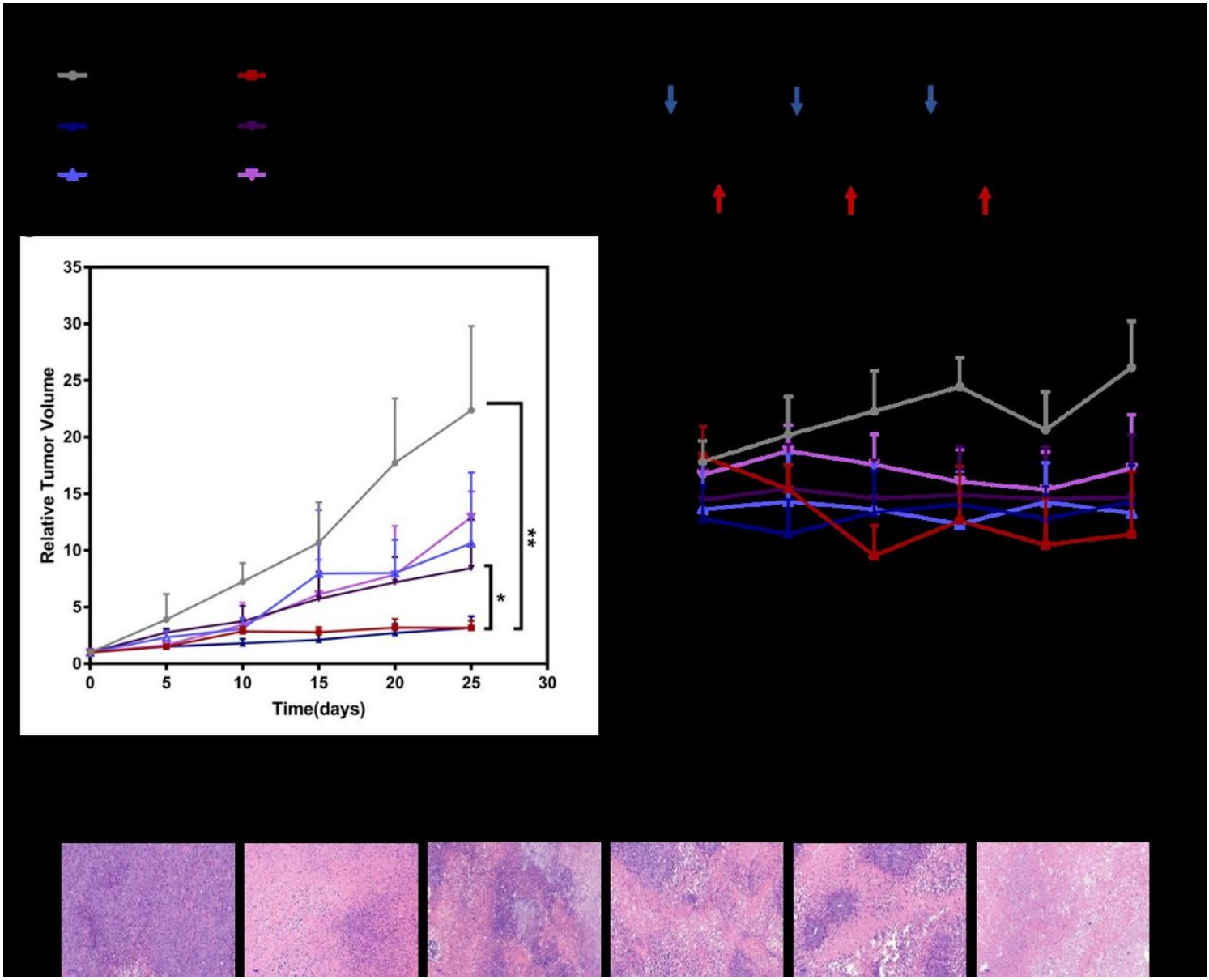

Figure 5

(A) The plasmid injection and drug injection schedule., respectively; (B) Groups during treatment; (C) Tumor growth curve after injected with various drug with 25 days,*p<0.05 and **p<0.01,vs Tf-LP/DOX (transfected group), n=5; (D) Body weight change curve of the mice; (E) Representative H&E sections of tumor tissue of mice after treatment with various drug.

Supplementary Files

This is a list of supplementary files associated with this preprint. Click to download.

- sup.jpg
- Supportinginformation.docx